

Correlated signals of first-order phase transitions and primordial black hole evaporation

Danny Marfatia¹ and Po-Yan Tseng²

¹ *Department of Physics & Astronomy, University of Hawaii at Manoa, 2505 Correa Rd., Honolulu, HI 96822, USA*

² *Department of Physics, National Tsing Hua University, 101 Kuang-Fu Rd., Hsinchu 300044, Taiwan R.O.C.*

ABSTRACT: Fermi balls produced in a cosmological first-order phase transition may collapse to primordial black holes (PBHs) if the fermion dark matter particles that comprise them interact via a sufficiently strong Yukawa force. We show that phase transitions described by a quartic thermal effective potential with vacuum energy, $0.1 \lesssim B^{1/4}/\text{MeV} \lesssim 10^3$, generate PBHs of mass, $10^{-20} \lesssim M_{\text{PBH}}/M_{\odot} \lesssim 10^{-16}$, and gravitational waves from the phase transition (at THEIA/ μ Ares) can be correlated with an isotropic extragalactic X-ray/ γ -ray background from PBH evaporation (at AMEGO-X/e-ASTROGAM).

Contents

1	Introduction	1
2	PBH formation	2
2.1	FB collapse to PBH	3
3	PBH evaporation spectra	4
4	Correlated signals	6
5	Summary	9
A	FB properties	9

1 Introduction

Primordial black holes (PBHs), hypothesized to have formed in the early Universe, are a good dark matter (DM) candidate [1–7]. They offer a compelling explanation [8–10] for the gravitational wave (GW) signals observed by LIGO/Virgo [11–13]. PBHs are typically thought to have been produced in the collapse of overdense regions developed from primordial inhomogeneities seeded by inflation [14, 15]. They may also form directly during a first-order phase transition (FOPT) [16–21], perhaps through bubble collisions.

In this work, we focus on a novel mechanism in which PBHs are produced in a FOPT through an intermediate step, wherein macroscopic Fermi balls (FBs) first form during the FOPT and subsequently collapse to PBHs [22]. FBs originate from the aggregation of fermion DM particles trapped in the false vacuum as the true vacuum bubbles expand [23–26]. The FOPT must take place in a dark sector because in the Standard Model (SM), the electroweak and quantum chromodynamics phase transitions are smooth crossovers. We consider the frequently arising quartic effective thermal potential to generate a FOPT. A Yukawa interaction with fermion DM will serve two purposes. The DM particle acquires an additional mass in the true vacuum, making it heavier than in the false vacuum [27]. Requiring the DM mass difference to be larger than the critical temperature of the FOPT, forces the DM particles to become trapped in the false vacuum. A DM-antiDM asymmetry then ensures that the shrinking volume of the false vacuum compresses the DM particles into FBs. Also, the attractive Yukawa force between DM particles causes the FBs to collapse to PBHs once its range becomes larger than the mean separation distance between particles in the FB [22].

Our goal is to show that in a certain mass range of PBHs, gravitational waves from the FOPT and the extragalactic X-ray and GeV γ -ray background from PBH evaporation

can be correlated. For $M_{\text{PBH}}/M_{\odot} \gtrsim 10^{-19}$, PBHs have lifetimes longer than the age of the Universe and are evaporating in the present epoch. PBH evaporation produces X-rays and GeV γ -rays that after redshifting are detectable at current (SPI, Fermi-LAT) and future (AMEGO-X, e-ASTROGAM) γ -ray telescopes [28–31]. The corresponding gravitational waves produced during the FOPT, are detectable at THEIA [32], and μ Ares [33].

The paper is organized as follows. We describe FB formation and the criteria for their collapse to PBHs in section 2. We outline our procedure for calculating the PBH evaporation spectra in section 3. In section 4, we scrutinize the input parameters of the effective potential by performing a parameter scan and calculate GW and extragalactic photon spectra for a few benchmark points. We summarize in section 5.

2 PBH formation

We consider the formation of PBHs via a two step process in the hidden sector. The dark Dirac fermion particles χ 's first aggregate to form macroscopic FBs during a dark scalar ϕ induced FOPT. Subsequently, the attractive Yukawa force between χ 's mediated by ϕ destabilizes the FBs which collapse to PBHs [22].

To realize the above scenario, we adopt a model defined by the Lagrangian,

$$\mathcal{L} \supset \bar{\chi}(i\cancel{\partial} - m)\chi - g_{\chi}\phi\bar{\chi}\chi - V_{\text{eff}}(\phi, T), \quad (2.1)$$

with the finite-temperature quartic effective potential [34, 35],

$$V_{\text{eff}}(\phi, T) = D(T^2 - T_0^2)\phi^2 - (AT + C)\phi^3 + \frac{\lambda}{4}\phi^4, \quad (2.2)$$

which induces a FOPT in the early Universe. When the temperature drops below the critical temperature T_c (defined by $V_{\text{eff}}(0, T_c) = V_{\text{eff}}(v_{\phi}(T_c), T_c)$), the Universe starts to transit from the false vacuum (with $\langle\phi\rangle = 0$) to the true vacuum (with $\langle\phi\rangle = v_{\phi}$). At zero temperature, we define $B \equiv |V_{\text{eff}}(\tilde{\phi}_+, 0)|$ as the vacuum energy density evaluated at the global minimum $\tilde{\phi}_+$ [24]. Since $V_{\text{eff}}(\phi = 0, T) = 0$, B is the energy density difference between the $\phi = 0$ and $\tilde{\phi}_+$ phases at zero temperature. We choose the input parameters to be

$$\lambda, A, B, C, D, \quad (2.3)$$

and treat the destabilization temperature T_0 as a derived quantity [24].

An analytical expression for the Euclidean action $S_3(T)/T$ for quartic potentials can be found in Ref. [35]. We use this to calculate the bubble nucleation rate per unit volume $\Gamma(T)$, and hence the fraction of space in the false vacuum $F(t)$ [24]. Since the dark sector is partially thermalized via gravitational interactions with the SM sector, the total radiation energy density is $\rho(T) = \frac{\pi^2}{30}g_*T_{\text{SM}}^4$, where $g_* = g_*^{\text{SM}} + g_*^{\text{D}}(T/T_{\text{SM}})^4$ is the total number of relativistic degrees of freedom when the dark and SM sectors are at temperatures T and T_{SM} , respectively, and $g_*^{\text{D}} = 4.5$ at all relevant times. We properly account for the amount of dark radiation after the FOPT by relating the effective number of extra neutrino species

contributed by the dark sector after the phase transition, ΔN_{eff} , to T/T_{SM} at the end of the FOPT [24].

We identify the phase transition temperature T_\star with the temperature of percolation, which we define as the temperature at which a fraction $1/e$ of the space is in the false vacuum. Then, the time of the phase transition t_\star is given by

$$F(t_\star) = 1/e \simeq 0.37. \quad (2.4)$$

As the FOPT proceeds, the false vacuum separates into smaller volumes. The formation of FBs in a *false vacuum bubble* at T_\star dominates over true vacuum bubble nucleation inside it when the false vacuum bubble reaches a critical volume V_\star given by $\Gamma(T_\star)V_\star R_\star \sim v_w$ [23]. Here, R_\star is the radius of the false vacuum bubble and v_w is the bubble wall velocity. Assuming that each critical volume results in one FB, the number density of FBs is determined by $n_{\text{FB}}|_{T_\star} V_\star = F(t_\star)$.

For stable FBs to exist in the false vacuum, during the phase transition there must be a nonzero asymmetry $\eta_\chi \equiv (n_\chi - n_{\bar{\chi}})/s$ in the number densities (where the entropy density is $s = (2\pi^2/45)(g_{\text{SM}}^{\text{SM}} T_{\text{SM}}^3 + g_{\text{SM}}^{\text{D}} T^3)$), so that a net number of particles remain after pair annihilation $\bar{\chi}\chi \rightarrow \phi\phi$, and χ must carry a conserved global $U(1)_Q$ so that Q -charge can be accumulated to stabilize a FB [23]. The net Q -charge trapped in a FB, which is equivalent to the total number of χ in a FB, is $Q_{\text{FB}} = \eta_\chi (s/n_{\text{FB}})_{T_\star}$. To be stable, the FBs must satisfy [27]

$$\frac{dM_{\text{FB}}}{dQ_{\text{FB}}} < m + g_\chi v_\phi(T), \quad \text{and} \quad \frac{d^2 M_{\text{FB}}}{dQ_{\text{FB}}^2} < 0.$$

Since a black hole violates continuous global symmetries, PBH formation via FB collapse will not conserve the Q -charge of the FB, and the PBH will evaporate as a Schwarzschild black hole.

Complete expressions for the energy, mass and radius of a FB are provided in appendix A. Note that if the Yukawa energy is negligible, then for $0.1 \leq B^{1/4}/\text{MeV} \leq 10^4$, the FB radius is typically much larger than the Schwarzschild radius of a FB, and the FB does not collapse to a PBH.

2.1 FB collapse to PBH

The χ 's inside a FB couple via the attractive Yukawa interaction $g_\chi \phi \bar{\chi}\chi$, with interaction length,

$$L_\phi(T) \equiv \left(\frac{d^2 V_{\text{eff}}}{d\phi^2} \Big|_{\phi=0} \right)^{-1/2} = (2D(T^2 - T_0^2))^{-1/2}. \quad (2.5)$$

The Yukawa potential energy contribution E_Y to the total FB energy in Eq. (A.1) is

$$E_Y \simeq -\frac{3g_\chi^2 Q_{\text{FB}}^2}{8\pi R} \left(\frac{L_\phi}{R} \right)^2. \quad (2.6)$$

As we can see, $L_\phi(T)$ and $|E_Y|$ increase as the temperature decreases. When $|E_Y|$ becomes larger than the Fermi-gas kinetic energy, the FB becomes unstable and starts collapsing to

a PBH. This coincides with L_ϕ becoming roughly the same as the mean separation distance of χ 's, i.e., $L_\phi \simeq R_{\text{FB}}/Q_{\text{FB}}^{1/3}$. More specifically, the temperature T_ϕ for PBH formation is given by [22]

$$L_\phi(T_\phi) = (2D(T_\phi^2 - T_0^2))^{-1/2} = \frac{1}{g_\chi} \sqrt{\frac{2\pi}{3\sqrt{3}}} \left(\frac{2\pi}{3}\right)^{1/6} \frac{R_{\text{FB}}}{Q_{\text{FB}}^{1/3}}. \quad (2.7)$$

For our energy scale of interest ($0.1 \leq B^{1/4}/\text{MeV} \leq 10^4$) we find $T_\star > T_\phi$, so that the FB forms first and then collapses to a PBH. Immediately after formation, the PBH mass is obtained by replacing T with T_ϕ in Eq. (A.4), i.e., $M_{\text{PBH}} = M_{\text{FB}}(T_\phi)$, and the number density is $n_{\text{PBH}} = n_{\text{FB}}|_{T_\star} s(T_\phi)/s(T_\star)$ due to the adiabatic evolution of the Universe [22]. Note that since the FBs have a monochromatic mass function, so do the PBHs. The PBH number density and relic abundance in the present Universe are given by [5]

$$\frac{n_{\text{PBH}}|_0}{s_0} = \left(\frac{n_{\text{PBH}}}{s}\right)_{T_\phi} = \frac{3}{4} \frac{T_\phi}{M_{\text{PBH}}} \frac{\rho_{\text{PBH}}(T_\phi)}{\rho(T_\phi)}, \quad (2.8)$$

$$\Omega_{\text{PBH}} h^2 = \frac{M_{\text{PBH}}|_0 n_{\text{PBH}}|_0}{3M_{\text{Pl}}^2 (H_0/h)^2}, \quad (2.9)$$

where the Hubble constant, $H_0 = 2.13h \times 10^{-42} \text{ GeV}$.

3 PBH evaporation spectra

The evaporation of a PBH produces a primary component of particles from Hawking emission and a secondary component from their decay and fragmentation. Hawking emission includes all particles with mass below the PBH temperature, regardless of their quantum numbers. A PBH emits primary particles thermally with temperature $T_{\text{PBH}} = M_{\text{Pl}}^2/M_{\text{PBH}}$, and numerically expressed as

$$T_{\text{PBH}} \simeq 5.3 \text{ MeV} \times \left(\frac{10^{-18} M_\odot}{M_{\text{PBH}}}\right). \quad (3.1)$$

For $M_{\text{PBH}}/M_\odot \lesssim 10^{-20}$, PBHs have evaporated before today. The emission rate of primary particle i is given by [36, 37]

$$\frac{dN_i}{dE dt} = \frac{n_i^{\text{d.o.f}} \Gamma_i(E, M_{\text{PBH}})}{2\pi(e^{E/T_{\text{PBH}}} \pm 1)}, \quad (3.2)$$

where $n_i^{\text{d.o.f}}$ is the number of degrees of freedom of particle i , the graybody factor $\Gamma_i(E, M)$ describes a wave packet scattering in the nontrivial PBH spacetime geometry from the PBH horizon to an observer at infinity, and the $+$ ($-$) in the denominator corresponds to fermions (bosons).

We restrict our study to photon emission because it provides the most severe model-independent constraints on our parameter space. In order to compare with observations, the secondary component of emitted particles must be carefully calculated. Particle decays, quarks hadronization and fragmentation have significant effects on the spectra at low

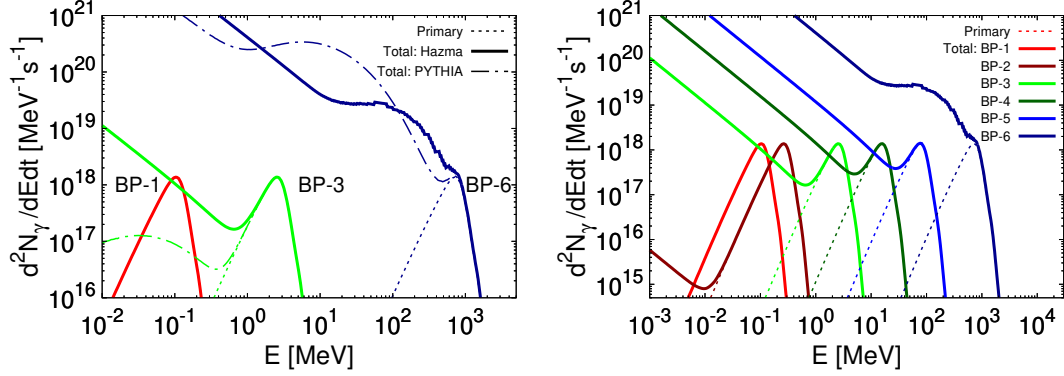


Figure 1. Left panel: Instantaneous photon spectra from PBH evaporation using BlackHawk with Hazma and with PYTHIA for three benchmark points. The Hazma and PYTHIA spectra are identical for **BP-1**, which has a relatively heavy PBH mass. Note the large differences in the secondary contributions for **BP-3** and **BP-6**. Right panel: The photon spectra for all six benchmark points in Table 1.

energies. In particular, secondary photons are produced in final state radiation from, and decays of, primary particles ($e^\pm, \mu^\pm, \pi^\pm, \pi^0$). We employ the software package BlackHawk v2.0 [38, 39] with Hazma [40, 41] to compute the photon spectra from PBH evaporation. In Fig. 1 we display a comparison between the instantaneous photon spectra using Hazma and PYTHIA [42]/HERWIG [43]. Clearly, the secondary components of the spectra are very different for PBHs lighter than $\sim 10^{-17}M_\odot$. The primary reason for this is that the PYTHIA/HERWIG hadronization procedure is not reliable below 5 GeV.

The differential full-sky extragalactic γ -ray background (EGB) flux due to PBH evaporation is given by [5]

$$\frac{d\Phi}{dE} = n_{\text{PBH}}|_0 \int_{t_{\text{CMB}}}^{\min(t_{\text{eva}}, t_0)} c[1+z(t)] \left. \frac{d^2N_\gamma}{d\tilde{E}dt} \right|_{\tilde{E}=[1+z(t)]E} dt. \quad (3.3)$$

If the PBHs have a lifetime shorter than the age of the Universe, $n_{\text{PBH}}|_0$ is interpreted as the number density today had the PBHs not evaporated. The lower limit of the integral is the time of last scattering, $t_{\text{CMB}} = 3.8 \times 10^5$ yr, after which photons propagate freely. The upper limit is the smaller of lifetime of the PBH (t_{eva}) and the age of the Universe ($t_0 = 13.77 \times 10^9$ yr). We approximate the evolution of the Universe as matter dominated until the current epoch, so that

$$1+z(t) = \left(\frac{t_0}{t}\right)^{2/3}. \quad (3.4)$$

From Eq. (2.8), it is convenient to define the commonly used parameter [5]

$$\beta' \equiv \gamma^{1/2} \left(\frac{g_*(T_\phi)}{106.75}\right)^{-1/4} \left(\frac{h}{0.67}\right)^{-2} \frac{\rho_{\text{PBH}}(T_\phi)}{\rho(T_\phi)}, \quad (3.5)$$

which is a measure of the fraction of the energy density of the Universe in PBHs at formation. We set $h = 0.67$. The parameter γ is defined by $M_{\text{PBH}} \equiv \gamma M_H$, where $M_H = c^3 t / G$

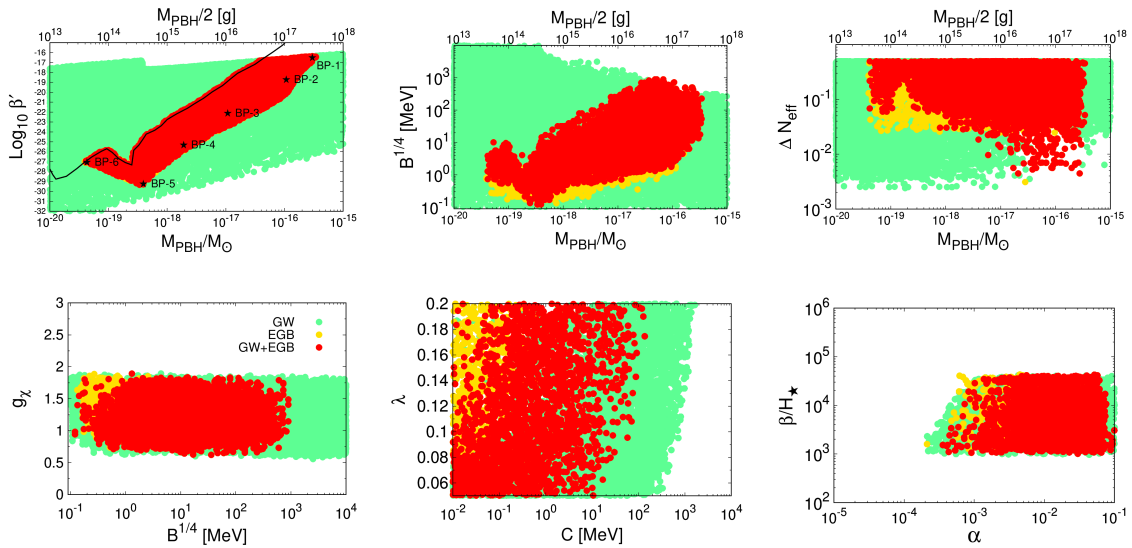


Figure 2. The regions of parameter space that produce a detectable diffuse extragalactic X-ray/ γ -ray background at the MeV γ -ray telescopes, AMEGO-X/e-ASTROGAM (yellow), and a gravitational wave signal at THEIA/ μ Ares (green). In the red regions both measurements can be made. The solid black curve in the top left panel is the current bound from observations of the extragalactic γ -ray background and from the damping of small scale CMB anisotropies. All points satisfy $\Omega_{\text{PBH}} h^2 \leq 0.12$ and $\Delta N_{\text{eff}} \leq 0.5$.

is the Hubble horizon mass in the radiation dominated era. We treat the definition of γ as a parametric relation with no connection to the dynamics of gravitational collapse. This is to enable us to use bounds presented in terms of β' . In our scenario, the prefactor in Eq. (3.5) is determined by the calculable quantities, M_{PBH} and T_ϕ :

$$\gamma^{1/2} \left(\frac{g_*(T_\phi)}{106.75} \right)^{-1/4} = 4.58 \times 10^{-12} \frac{T_\phi}{\text{MeV}} \left(\frac{M_{\text{PBH}}}{10^{-18} M_\odot} \right)^{1/2}. \quad (3.6)$$

We consider two types of bounds on β' . The diffuse extragalactic γ -ray background measured by HEAO-1, COMPTEL, EGRET and Fermi-LAT places a strong, secure bound for $10^{-19} \lesssim M_{\text{PBH}}/M_\odot \lesssim 10^{-15}$ [5]. The damping of small scale CMB anisotropies by PBH evaporation after recombination places the most stringent constraints on PBHs with mass $10^{-20} \lesssim M_{\text{PBH}}/M_\odot \lesssim 10^{-19}$ [44]. The combined bound is shown in the $(M_{\text{PBH}}/M_\odot, \beta')$ panel of Fig. 2 as a solid black curve.

4 Correlated signals

We scan the parameters of the effective potential in Eq. (2.3), the temperature ratio of the dark and SM sectors $T_*/T_{\text{SM}*}$ during the phase transition, the Yukawa coupling g_χ , and

Table 1. Benchmark points with $A = 0.1$ fixed. T_f is the temperature of the dark sector after the FOPT. α is the strength of the transition, defined by the ratio of the latent heat released and the radiation energy density at the time of the FOPT, and β is the inverse duration of the phase transition.

	BP-1	BP-2	BP-3	BP-4	BP-5	BP-6
λ	0.061	0.110	0.195	0.087	0.150	0.158
$B^{1/4}/\text{MeV}$	75.14	13.81	1.501	1.261	0.121	2.999
C/MeV	0.249	0.462	0.078	0.052	0.011	0.325
D	0.596	1.458	1.119	0.596	1.418	0.519
g_χ	1.088	1.301	1.011	1.289	0.983	1.228
η_χ	1.03×10^{-9}	1.28×10^{-10}	1.64×10^{-12}	1.21×10^{-15}	2.59×10^{-18}	6.26×10^{-17}
m/MeV	53.41	0.120	0.259	0.394	0.341	1.704
$T_{\text{SM}\star}/\text{MeV}$	94.68	14.63	0.895	2.104	0.164	4.774
T_\star/MeV	53.16	6.143	0.421	0.868	0.052	2.287
T_f/MeV	59.63	6.888	0.472	1.023	0.068	2.571
T_ϕ/MeV	53.09	6.045	0.415	0.857	0.050	1.950
$S_3(T_\star)/T_\star$	155	159	166	171	180	170
M_{PBH}/M_\odot	2.92×10^{-16}	1.15×10^{-16}	1.19×10^{-17}	1.93×10^{-18}	3.91×10^{-19}	4.23×10^{-20}
Q_{FB}	1.26×10^{42}	4.31×10^{42}	5.96×10^{42}	5.01×10^{41}	7.58×10^{41}	4.18×10^{39}
β'	2.80×10^{-17}	2.54×10^{-19}	7.78×10^{-23}	4.45×10^{-26}	5.75×10^{-30}	8.97×10^{-28}
α	1.48×10^{-2}	7.40×10^{-3}	1.20×10^{-2}	1.12×10^{-2}	1.35×10^{-2}	1.30×10^{-2}
β/H_\star	4.41×10^3	9.36×10^3	3.21×10^4	3.25×10^3	4.94×10^3	2.64×10^3
v_w	0.904	0.904	0.904	0.930	0.963	0.905
$v_\phi(T_\star)/\text{MeV}$	224	23.1	1.426	3.821	0.247	8.157
$dM_{\text{FB}}/dQ_{\text{FB}}/\text{MeV}$	258	28.3	1.980	4.264	0.573	10.89
$\Omega_{\text{PBH}}h^2$	0.079	1.12×10^{-3}	1.09×10^{-6}	1.52×10^{-9}	2.15×10^{-13}	6.35×10^{-29}
ΔN_{eff}	0.218	0.126	0.208	0.146	0.147	0.221

the bare mass m in the ranges,

$$\begin{aligned}
0.05 \leq \lambda \leq 0.2, \quad 0.1 \leq B^{1/4}/\text{MeV} \leq 10^4, \quad 0.01 \leq C/\text{MeV} \leq 10^4, \\
0.1 \leq D \leq 10, \quad 0.3 \leq T_\star/T_{\text{SM}\star} \leq 1.0, \quad 0.01 \leq g_\chi \leq \sqrt{4\pi}, \\
10^{-3} \leq m/B^{1/4} \leq 10.
\end{aligned}
\tag{4.1}$$

We fix $A = 0.1$ and adjust the value of the asymmetry parameter η_χ to ensure that $\Omega_{\text{PBH}}h^2 \leq \Omega_{\text{DM}}h^2 \simeq 0.12$. The results are shown in Fig. 2. In the green regions, GW signals from the FOPT are detectable by the proposed THEIA [32], and μAres [33] telescopes. In the yellow regions, PBH evaporation produces an extragalactic X-ray/ γ -ray background that can be probed by future (AMEGO-X, e-ASTROGAM) and current (SPI, Fermi-LAT) γ -ray telescopes [28, 29]. In the red regions, both the EGB and GWs can be observed.

We select six benchmark points that lie in the red regions and that are compatible with the EGB and CMB bounds. They are marked in the upper left panel of Fig. 2 and listed in Table 1. Their GW spectra, arising from sound waves in the plasma during the FOPT, are shown in Fig. 3; for the procedure used, see Ref. [45]. μAres is sensitive to all benchmark points except **BP-5**, which can be detected by THEIA. We have also found points that can be detected by both μAres and THEIA. The corresponding EGBs are shown in Fig. 4. Our benchmark points are selected to yield an observable EGB at

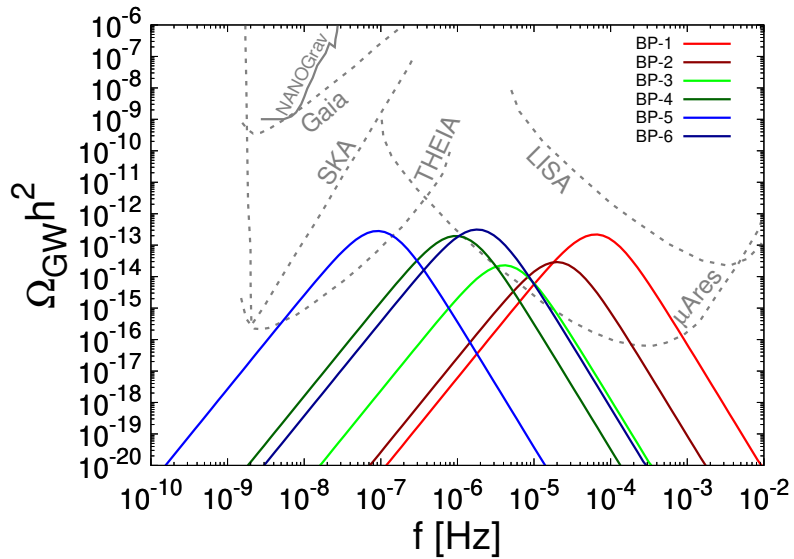


Figure 3. Gravitational wave power spectra for the benchmark points in Table 1.

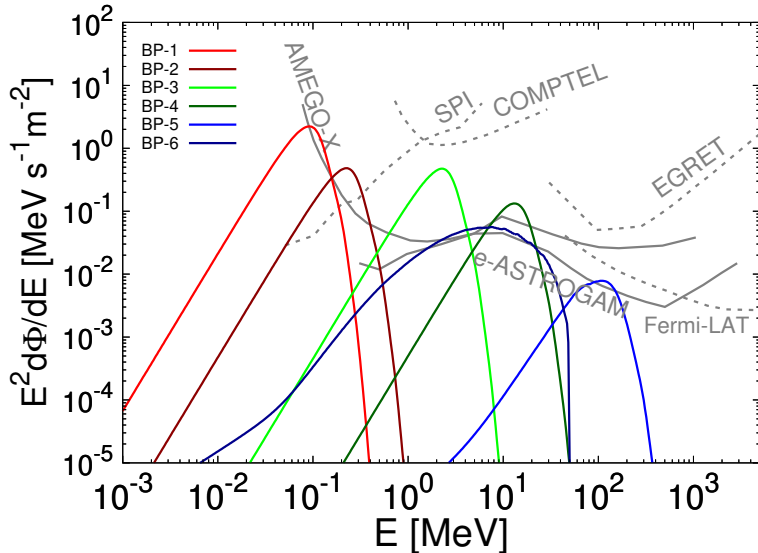


Figure 4. Extragalactic γ -ray spectra from PBH evaporation for the benchmark points in Table 1.

the proposed AMEGO-X and e-ASTROGAM telescopes. The 3σ sensitivities, including those of the past and current telescopes, SPI, COMPTEL, EGRET, and Fermi-LAT are shown. The spectral shape of **BP-6** is different from that of the other points because in the instantaneous photon spectrum in Fig. 1, the sharp peak expected from Hawking emission is washed out by secondary emission. Note that only **BP-1** has $\Omega_{\text{PBH}} h^2 \sim \Omega_{\text{DM}} h^2$, and that the relic density of **BP-6** is vanishingly small because the PBHs have a much shorter lifetime ($\sim 10^7$ yr) than the age of the Universe.

5 Summary

We studied a novel mechanism of PBH formation, in which macroscopic Fermi balls produced during a FOPT in a dark sector become unstable and collapse to PBHs. In the framework of a generic thermal effective potential, if the difference in vacuum energy at zero temperature is $0.1 \lesssim B^{1/4}/\text{MeV} \lesssim 10^4$, PBHs of mass $10^{-20}M_\odot \lesssim M_{\text{PBH}} \lesssim 10^{-15}M_\odot$ are produced.

For $3 \times 10^{-20}M_\odot \lesssim M_{\text{PBH}} \lesssim 3 \times 10^{-16}M_\odot$, the stochastic background of gravitational waves from the FOPT that peaks in the $10^{-7} \text{ Hz} - 10^{-4} \text{ Hz}$ range can be detected at the proposed THEIA and μAres telescopes, and in correlation, a substantial extragalactic X-ray/ γ -ray background produced by PBH evaporation can be detected at SPI, Fermi-LAT, and the proposed MeV γ -ray telescopes, AMEGO-X and e-ASTROGAM; see Figs. 3 and 4. A measurable amount of dark radiation is also typically expected; see Fig. 2.

Acknowledgements

We thank A. Arbey and J. Auffinger for help with the BlackHawk package. D.M. is supported in part by the U.S. DOE under Grant No. de-sc0010504.

A FB properties

We derive analytic expressions for the FB mass and radius. Including the Fermi gas kinetic energy, Yukawa potential energy, and the temperature-dependent potential energy difference between the false and true vacua, the energy of a FB of radius R , temperature T , and charge Q_{FB} , can be approximately written as [22]

$$E_{\text{FB}} = \frac{3\pi}{4} \left(\frac{3}{2\pi}\right)^{2/3} \frac{Q_{\text{FB}}^{4/3}}{R} \left[1 + \frac{4\pi}{9} \left(\frac{2\pi}{3}\right)^{1/3} \frac{R^2 T^2}{Q_{\text{FB}}^{2/3}} \left(1 + \frac{3}{2\pi^2} \frac{m^2}{T^2}\right) \right] - \frac{3g_\chi^2}{8\pi} \frac{Q_{\text{FB}}^2 L_\phi^2}{R^3} + \frac{4\pi}{3} V_0 R^3 \left(1 + \frac{T^2 m^2}{12V_0}\right), \quad (\text{A.1})$$

where $V_0(T) \equiv V_{\text{eff}}(0, T) - V_{\text{eff}}(v_\phi(T), T)$, which at zero temperature is B . Since the FB is a macroscopic object, a contribution from the surface tension is negligible.

To find R_{FB} , we require $dE_{\text{FB}}/dR = 0$, which yields the cubic equation,

$$(R^2)^3 + a_2(R^2)^2 + a_1(R^2) + a_0 = 0, \quad (\text{A.2})$$

where

$$\begin{aligned} a_2 &\equiv \frac{\pi}{12} \left(\frac{3}{2\pi}\right)^{1/3} \frac{Q_{\text{FB}}^{2/3} T^2}{V_0} \left(1 + \frac{3}{2\pi^2} \frac{m^2}{T^2}\right) \left(1 + \frac{T^2 m^2}{12V_0}\right)^{-1}, \\ a_1 &\equiv -\frac{3}{16} \left(\frac{3}{2\pi}\right)^{2/3} \frac{Q_{\text{FB}}^{4/3}}{V_0} \left(1 + \frac{T^2 m^2}{12V_0}\right)^{-1}, \\ a_0 &\equiv \frac{9g_\chi^2}{32\pi^2} \frac{Q_{\text{FB}}^2 L_\phi^2}{V_0} \left(1 + \frac{T^2 m^2}{12V_0}\right)^{-1}. \end{aligned} \quad (\text{A.3})$$

The largest of the three roots, $R_{\text{FB}}^2 = 2\sqrt{q} \cos \theta - a_2/3$, gives the FB radius [46]. Then evaluating E_{FB} at R_{FB} gives the mass of the FB. We find

$$\begin{aligned}
R_{\text{FB}} &= Q_{\text{FB}}^{1/3} \left[\frac{1}{4} \left(\frac{3}{2\pi} \right)^{2/3} \frac{1}{V_0} \right]^{1/4} X^{1/2}, \\
M_{\text{FB}} &= \frac{3}{4} Q_{\text{FB}} (9\pi^2 V_0)^{1/4} X^{-3/2} \\
&\quad \times \left\{ X + \frac{4}{9} \left(1 + \frac{T^2 m^2}{12V_0} \right) X^3 + \left(\frac{2\pi}{9} \frac{T^2}{V_0^{1/2}} + \frac{1}{3\pi} \frac{m^2}{V_0^{1/2}} \right) X^2 - \frac{2g_\chi^2 L_\phi^2 V_0^{1/2}}{3\pi} \right\},
\end{aligned} \tag{A.4}$$

where X is defined as [46]

$$\begin{aligned}
X &\equiv \left[\left(1 + \frac{13}{108} \frac{T^2 m^2}{V_0} + \frac{\pi^2 T^4}{81 V_0} + \frac{1}{36\pi^2} \frac{m^4}{V_0} \right)^{1/2} \cos \theta - \frac{\pi}{18} \frac{T^2}{V_0^{1/2}} \left(1 + \frac{3}{2\pi^2} \frac{m^2}{T^2} \right) \right] \left(1 + \frac{T^2 m^2}{12V_0} \right)^{-1}, \\
\theta &\equiv \frac{1}{3} \cos^{-1} \frac{r}{q^{3/2}}, \quad \text{with} \\
r &\equiv \frac{1}{6} (a_1 a_2 - 3a_0) - \frac{1}{27} a_2^3 \\
&= -\frac{1}{256} \frac{Q_{\text{FB}}^2 T^2}{V_0^2} \left(1 + \frac{T^2 m^2}{12V_0} \right)^{-3} \\
&\quad \times \left[\left(1 + \frac{3}{2\pi^2} \frac{m^2}{T^2} \right) \left(1 + \frac{35}{324} \frac{T^2 m^2}{V_0} + \frac{2\pi^2 T^4}{243 V_0} + \frac{1}{54\pi^2} \frac{m^4}{V_0} \right) + \frac{36g_\chi^2 L_\phi^2 V_0}{\pi^2 T^2} \left(1 + \frac{T^2 m^2}{12V_0} \right)^2 \right], \\
q &\equiv -\frac{1}{3} a_1 + \frac{1}{9} a_2^2 = \frac{1}{16} \left(\frac{3}{2\pi} \right)^{2/3} \frac{Q_{\text{FB}}^{4/3}}{V_0} \left(1 + \frac{13}{108} \frac{T^2 m^2}{V_0} + \frac{\pi^2 T^4}{81 V_0} + \frac{1}{36\pi^2} \frac{m^4}{V_0} \right) \left(1 + \frac{T^2 m^2}{12V_0} \right)^{-2}.
\end{aligned} \tag{A.5}$$

From the definition of θ , a solution exists only if $|r/q^{3/2}| \leq 1$. If we neglect the Yukawa energy, i.e., set $a_0 = 0$, and Taylor expand $\cos \theta \simeq \frac{\sqrt{3}}{2} + \frac{r}{6q^{3/2}}$, we find

$$\begin{aligned}
\cos \theta &\simeq \frac{\sqrt{3}}{2} - \frac{\pi}{36} \frac{T^2}{V_0^{1/2}} \left(1 + \frac{3}{2\pi^2} \frac{m^2}{T^2} \right) \left(1 + \frac{35}{324} \frac{T^2 m^2}{V_0} + \frac{2\pi^2 T^4}{243 V_0} + \frac{1}{54\pi^2} \frac{m^4}{V_0} \right) \\
&\quad \times \left(1 + \frac{13}{108} \frac{T^2 m^2}{V_0} + \frac{\pi^2 T^4}{81 V_0} + \frac{1}{36\pi^2} \frac{m^4}{V_0} \right)^{-3/2}, \\
X &\simeq \frac{\sqrt{3}}{2} \left(1 + \frac{T^2 m^2}{12V_0} \right)^{-1} \left(1 + \frac{13}{108} \frac{T^2 m^2}{V_0} + \frac{\pi^2 T^4}{81 V_0} + \frac{1}{36\pi^2} \frac{m^4}{V_0} \right)^{-1} \\
&\quad \times \left\{ \left(1 + \frac{13}{108} \frac{T^2 m^2}{V_0} + \frac{\pi^2 T^4}{81 V_0} + \frac{1}{36\pi^2} \frac{m^4}{V_0} \right)^{3/2} \right. \\
&\quad \left. - \left(\frac{\pi}{6\sqrt{3}} \frac{T^2}{V_0^{1/2}} + \frac{1}{4\sqrt{3}\pi} \frac{m^2}{V_0^{1/2}} \right) \left(1 + \frac{113}{972} \frac{T^2 m^2}{V_0} + \frac{8\pi^2 T^4}{729 V_0} + \frac{2}{81\pi^2} \frac{m^4}{V_0} \right) \right\} \\
&\simeq \frac{\sqrt{3}}{2} \left(1 - \frac{1}{4\sqrt{3}\pi} \frac{m^2}{V_0^{1/2}} - \frac{\pi}{6\sqrt{3}} \frac{T^2}{V_0^{1/2}} - \frac{5}{216} \frac{m^2 T^2}{V_0} \right).
\end{aligned} \tag{A.6}$$

In the limit, $V_0^{1/2} \gg T^2, m^2$, Eq. (A.4) can be simplified to

$$\begin{aligned}
R_{\text{FB}} &= Q_{\text{FB}}^{1/3} \left[\frac{3}{16} \left(\frac{3}{2\pi} \right)^{2/3} \frac{1}{V_0} \right]^{1/4} \left(1 - \frac{1}{8\sqrt{3}\pi} \frac{m^2}{V_0^{1/2}} - \frac{\pi}{12\sqrt{3}} \frac{T^2}{V_0^{1/2}} - \frac{5}{432} \frac{m^2 T^2}{V_0} \right), \\
M_{\text{FB}} &= Q_{\text{FB}} (12\pi^2 V_0)^{1/4} \left(1 + \frac{\sqrt{3}}{8\pi} \frac{m^2}{V_0^{1/2}} + \frac{\pi}{4\sqrt{3}} \frac{T^2}{V_0^{1/2}} - \frac{1}{16} \frac{m^2 T^2}{V_0} \right). \tag{A.7}
\end{aligned}$$

References

- [1] S. Hawking, *Mon. Not. Roy. Astron. Soc.* **152**, 75 (1971).
- [2] G. F. Chapline, *Nature* **253**, no.5489, 251-252 (1975).
- [3] M. Y. Khlopov, *Res. Astron. Astrophys.* **10**, 495-528 (2010), [arXiv:0801.0116 [astro-ph]].
- [4] B. Carr, F. Kuhnel and M. Sandstad, *Phys. Rev. D* **94**, no.8, 083504 (2016), [arXiv:1607.06077 [astro-ph.CO]].
- [5] B. Carr, K. Kohri, Y. Sendouda and J. Yokoyama, *Rept. Prog. Phys.* **84**, no.11, 116902 (2021) [arXiv:2002.12778 [astro-ph.CO]].
- [6] B. Carr and F. Kuhnel, *Ann. Rev. Nucl. Part. Sci.* **70**, 355-394 (2020), [arXiv:2006.02838 [astro-ph.CO]].
- [7] A. M. Green and B. J. Kavanagh, *J. Phys. G* **48**, no.4, 043001 (2021), [arXiv:2007.10722 [astro-ph.CO]].
- [8] S. Clesse and J. García-Bellido, *Phys. Dark Univ.* **15**, 142-147 (2017), [arXiv:1603.05234 [astro-ph.CO]].
- [9] S. Bird, I. Cholis, J. B. Muñoz, Y. Ali-Haïmoud, M. Kamionkowski, E. D. Kovetz, A. Raccanelli and A. G. Riess, *Phys. Rev. Lett.* **116**, no.20, 201301 (2016), [arXiv:1603.00464 [astro-ph.CO]].
- [10] M. Sasaki, T. Suyama, T. Tanaka and S. Yokoyama, *Phys. Rev. Lett.* **117**, no.6, 061101 (2016) [erratum: *Phys. Rev. Lett.* **121**, no.5, 059901 (2018)], [arXiv:1603.08338 [astro-ph.CO]].
- [11] B. P. Abbott *et al.* [LIGO Scientific and Virgo], *Phys. Rev. Lett.* **116**, no.6, 061102 (2016), [arXiv:1602.03837 [gr-qc]].
- [12] B. P. Abbott *et al.* [LIGO Scientific and Virgo], *Phys. Rev. Lett.* **116**, no.24, 241103 (2016), [arXiv:1606.04855 [gr-qc]].
- [13] B. P. Abbott *et al.* [LIGO Scientific and VIRGO], *Phys. Rev. Lett.* **118**, no.22, 221101 (2017) [erratum: *Phys. Rev. Lett.* **121**, no.12, 129901 (2018)], [arXiv:1706.01812 [gr-qc]].
- [14] B. J. Carr and S. W. Hawking, *Mon. Not. Roy. Astron. Soc.* **168**, 399-415 (1974)
- [15] M. Sasaki, T. Suyama, T. Tanaka and S. Yokoyama, *Class. Quant. Grav.* **35**, no.6, 063001 (2018), [arXiv:1801.05235 [astro-ph.CO]].
- [16] S. W. Hawking, I. G. Moss and J. M. Stewart, *Phys. Rev. D* **26**, 2681 (1982).
- [17] I. G. Moss, *Phys. Rev. D* **50**, 676-681 (1994).
- [18] R. V. Konoplich, S. G. Rubin, A. S. Sakharov and M. Y. Khlopov, *Phys. Atom. Nucl.* **62**, 1593-1600 (1999).
- [19] H. Kodama, M. Sasaki and K. Sato, *Prog. Theor. Phys.* **68**, 1979 (1982).
- [20] C. Gross, G. Landini, A. Strumia and D. Teresi, *JHEP* **09**, 033 (2021) [arXiv:2105.02840 [hep-ph]].
- [21] M. J. Baker, M. Breitbach, J. Kopp and L. Mittnacht, [arXiv:2105.07481 [astro-ph.CO]].
- [22] K. Kawana and K. P. Xie, *Phys. Lett. B* **824**, 136791 (2022) [arXiv:2106.00111 [astro-ph.CO]].

- [23] J. P. Hong, S. Jung and K. P. Xie, Phys. Rev. D **102**, no. 7, 075028 (2020), [arXiv:2008.04430 [hep-ph]].
- [24] D. Marfatia and P. Y. Tseng, JHEP **11**, 068 (2021), [arXiv:2107.00859 [hep-ph]].
- [25] E. Witten, Phys. Rev. D **30**, 272 (1984).
- [26] Y. Bai, A. J. Long and S. Lu, Phys. Rev. D **99**, no. 5, 055047 (2019), [arXiv:1810.04360 [hep-ph]].
- [27] P. Huang and K. P. Xie, Phys. Rev. D **105**, no.11, 115033 (2022) [arXiv:2201.07243 [hep-ph]].
- [28] A. De Angelis *et al.* [e-ASTROGAM], JHEAp **19**, 1-106 (2018), [arXiv:1711.01265 [astro-ph.HE]].
- [29] H. Fleischhack, PoS **ICRC2021**, 649 (2021), [arXiv:2108.02860 [astro-ph.IM]].
- [30] R. Laha, J. B. Muñoz and T. R. Slatyer, Phys. Rev. D **101**, no.12, 123514 (2020), [arXiv:2004.00627 [astro-ph.CO]].
- [31] M. Ackermann *et al.* [Fermi-LAT], Astrophys. J. **857**, no.1, 49 (2018) [arXiv:1802.00100 [astro-ph.HE]].
- [32] The THEIA Collaboration, [arXiv:1707.01348 [astro-ph.IM]].
- [33] A. Sesana, N. Korsakova, M. A. Sedda, V. Baibhav, E. Barausse, S. Barke, E. Berti, M. Bonetti, P. R. Capelo and C. Caprini, *et al.* Exper. Astron. **51**, no.3, 1333-1383 (2021) [arXiv:1908.11391 [astro-ph.IM]].
- [34] M. Dine, R. G. Leigh, P. Y. Huet, A. D. Linde and D. A. Linde, Phys. Rev. D **46**, 550-571 (1992) [arXiv:hep-ph/9203203 [hep-ph]].
- [35] F. C. Adams, Phys. Rev. D **48**, 2800 (1993), [hep-ph/9302321].
- [36] S. W. Hawking, Nature **248**, 30-31 (1974).
- [37] S. W. Hawking, Commun. Math. Phys. **43**, 199-220 (1975).
- [38] A. Arbey and J. Auffinger, Eur. Phys. J. C **79**, no.8, 693 (2019), [arXiv:1905.04268 [gr-qc]].
- [39] A. Arbey and J. Auffinger, Eur. Phys. J. C **81**, 10 (2021) [arXiv:2108.02737 [gr-qc]].
- [40] A. Coogan, L. Morrison and S. Profumo, JCAP **01**, 056 (2020) [arXiv:1907.11846 [hep-ph]].
- [41] A. Coogan, L. Morrison and S. Profumo, Phys. Rev. Lett. **126**, no.17, 171101 (2021), [arXiv:2010.04797 [astro-ph.CO]].
- [42] T. Sjöstrand, S. Ask, J. R. Christiansen, R. Corke, N. Desai, P. Ilten, S. Mrenna, S. Prestel, C. O. Rasmussen and P. Z. Skands, Comput. Phys. Commun. **191**, 159-177 (2015) [arXiv:1410.3012 [hep-ph]].
- [43] J. Bellm, G. Bewick, S. Ferrario Ravasio, S. Gieseke, D. Grellscheid, P. Kirchgaßer, M. R. Masouminia, G. Nail, A. Papaefstathiou and S. Platzer, *et al.* Eur. Phys. J. C **80**, no.5, 452 (2020) [arXiv:1912.06509 [hep-ph]].
- [44] B. J. Carr, K. Kohri, Y. Sendouda and J. Yokoyama, Phys. Rev. D **81**, 104019 (2010), [arXiv:0912.5297 [astro-ph.CO]].
- [45] D. Marfatia and P. Y. Tseng, JHEP **02**, 022 (2021) [arXiv:2006.07313 [hep-ph]].
- [46] T. Han, D. Marfatia and R. J. Zhang, Phys. Rev. D **61**, 013007 (2000), [arXiv:hep-ph/9906508 [hep-ph]].